Journal of Optoelectronics and Advanced Materials Vol. 5, No. 3, September 2003, p. 589 - 597

INFLUENCE OF IMPURITIES ON THE GROWTH KINETIC OF KDP

H. V. Alexandru*, C. Berbecaru, R. C. Radulescu[a], F. Stanculescu, B. Logofatu

University of Bucharest, Faculty of Physics, Bucharest, Romania
[a]Galway-Mayo Institute of Technology, Dublin Road, Galway, Ireland

Growth kinetic of prismatic faces of KDP crystals in impure solutions were measured and analyzed. Two dimensional (2D) heterogeneous nucleation mechanism of growth was found to dominate at higher supersaturations, where the surface coverage of ad-molecules $\theta \sim 10^{-6}$ is about of the same order of magnitude as impurity concentration in solution. At smaller supersaturations the dislocation mechanism of growth is severely retarded by the stopper action of impurities. At the limit of the "dead" growth zone, the much higher critical coverage $\theta^* \sim 10^{-3}$ suggest the segregation coefficient of impurities increases dramatically at lower supersaturations. The influence of solution pH was discussed and the lower limit of adsorption energy of impurities (15 ÷ 18) kcal/mol was estimated.

(Received August 12, 2003; accepted August 28, 2003)

Keywords: Inorganic compound, Interfaces, Crystal growth, Thermodynamic properties

1. Introduction

Potassium dihydrogen phosphate crystal (KDP) with the chemical formula KH_2PO_4 is a non-linear optical material of high damage threshold in high power laser beams [1]. It is used for frequency conversion in laser nuclear fusion experiments and fast growing methods were developed for very large crystals [2-3]. Optical distortions in rapidly grown KDP and DKDP (deuterated isomorph of KDP) crystals were not larger than in the usual ones [4,5]. Improvements in the method of rapid growth were made by continuous filtration and overheating of solution [6]. A large number of papers were devoted to the growth kinetic analysis of prismatic and pyramidal faces of KDP [7-16]. The influence of impurities on the growth kinetic was also presented [17-20].

The laser damage threshold of non-linear optical crystals used for frequency conversion: Q-switches, parametric oscillators, etc, depends on the growth imperfections (dislocations, growth inclusions) and the concentration of impurities. "Poison" impurities for the prismatic faces of KDP are Cr^{3+}, Fe^{3+}, Al^{3+} like metals. Greenish color of crystals shows an increased content of such metals, which substantially decreases the damage threshold of optical components [21]. Prismatic faces are much more sensitive to Me^{3+} impurities than the pyramidal faces. The segregation coefficient of Me^{3+} impurities is sensitive to the solution pH and highly dependent on supersaturation [20,22]. A "dead" growth zone appears at smaller supersaturations, even in nominally "pure" solutions [23,24].

Heterogeneous 2D nucleation mechanism was found to be active on the prismatic faces of KDP in impure (Fe^{3+}) solutions, at $\sigma > (6–8)\ 10^{-2}$ [14]. Evidences about the surface diffusion mechanism of growth and 2D nucleation mechanism, which occur at $\sigma > 5 \times 10^{-2}$ was found in AFM ex-situ studies of pyramidal faces of KDP [25].

The purpose of this paper is to analyze the dual action of impurities as promoters of 2D–heterogeneous nucleation mechanism of growth at higher supersaturations and as retarding factor at smaller supersaturations, along with some thermodynamic growth parameters estimation.

* Corresponding author: horia@alpha1.infim.ro

2. Experimental data

Growth experiments were performed in dynamic regime. Fractional recrystallisation procedure [26-28] was used in order to improve the purity of the basic substance. Middle fraction of recrystallised product was used in experiments. KDP crystals were grown in dynamic regime, by the reversible rotation of the "tree" crystal support system at 40-70 rpm (10–20 seconds rotation in one direction and 2-4 seconds break), under the electronic control of the leading engine [13-15]. Fully transparent crystallisation system was used, which allowed following in situ the dimensions of the three crystals simultaneously grown in the same conditions. Details about the experimental arrangement were presented in ref. [20]. In short, three crystals of 8-10 cm (see Fig. 1) were grown with Z axis in horizontal position and the crystal thickness along <110> direction were measured with a vertical cathetometer (± 0.01 mm). Mean value of the growth rate $R^{\langle 100\rangle}(\sigma)$ of the four prismatic faces of every crystal was estimated as $R^{\langle 100\rangle} = R^{\langle 110\rangle}/\sqrt{2}$. Considering 4 cm crystal rotation radius and 60 rpm rotation speed, the solution velocity exceeds 20 cm/sec at the apexes. A maximum value of KDP growth rate is usually attained at solution velocities higher than (5 ÷ 10) cm/sec (see Fig. 6 in ref [41] and Fig. 6 in ref. [42]). This way, the kinetic regime of growth was insured.

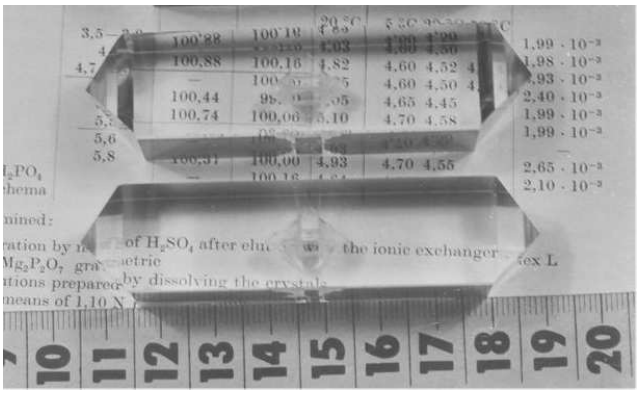

Fig.1. KDP crystals grown in the experiment corresponding to the kinetic curve III in Fig. 2.

Table 1. Characteristic constants in eq. $R = R_1\,\sigma^{\,m}$ at higher supersaturations in Figs. 2 and 3.

Curve Fig.1	$10^6 \cdot R_1$ (m/s)	m	r (%)
(II)	6.32_3	1.85_6	99.5_2
(III)	3.18_5	1.68_3	98.9_0
(IV)	2.86_5	1.93_9	99.9_1

Z-cut slices, from a good quality crystal, were shaped close to the natural habit of the crystal and were used as seeds. Seeds regeneration (natural habit reconstruction), was accomplished in a few hours, using higher supersaturations in the growth regime, against all literature prescriptions [22].

The temperature program was implemented with a Pt 100 thermometer (± 0.01 ^{o}C), a microcomputer and a phase control power regulator [29]. Solubility and supersaturation control were presented in ref. [14]. Typical grown crystals are presented in Fig. 1.

3. Growth kinetic analysis

We present some typical growth kinetic data R(σ) in Fig. 2. Data for the curve (II) was drawn from ref. [23] for "pure" KDP substance, crystals grown at 30 ^{o}C. Curve (III) represents our kinetic

data for crystals grown at 52 °C and pH 4.6, from purified substance by fractional recrystallisation (residual Fe^{3+} impurities about 5 ppm). Curve (IV) correspond also to our data in normal pH solutions at 40 °C, with Fe^{3+} ~ 20 ppm and no detectable Cr^{3+} traces. There are three distinct regions of growth kinetic in Fig. 2. At higher supersaturations apparently a parabolic dependence is valid, followed by an intermediate region at smaller supersaturations and a "dead" growth zone, were no growth occur, or the growth rate is too small to be detected in usual conditions.

In Fig. 3 the same growth kinetic data R(σ) were represented in double log scale. At higher supersaturations a good fit of data is given by the empirical equation:

$$R = R_1 \, \sigma^{m} \tag{1}$$

were constants R_1 and m are given in Table 1, with a good correlation factor. The value of the exponent $1 < m < 2$ suggest a BCF [30] (surface diffusion) equation might be valid.

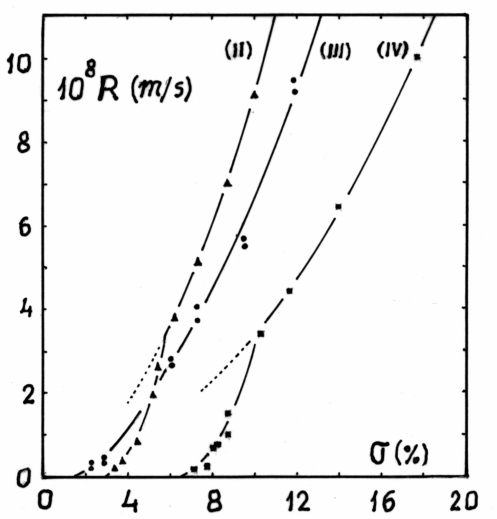

Fig. 2. Growth kinetic data for the prismatic faces of KDP. Data on the curve (II) was drawn from ref. [23]. The couples of the filled circles on the curve (III) show the extreme values among the three crystals, grown simultaneously in the same conditions. In that experiment the basic substance used was refined by fractional recrystallisation, and crystals were grown at pH 4.8. Curve (IV) corresponds to crystals grown from solution with ~20 ppm Fe^{3+} impurity (see text).

In the intermediate region of growth, dashed lines in Fig. 3 have no significance and shall be further discussed. Similar growth kinetic curves of the prismatic faces of KDP in solutions impurified with ethylene were obtained on a large supersaturation range in ref. [19]. However, according to the authors [19], even in "nominally pure" solution the lower intermediate zone of growth appears like in our Fig.2. This is probably due to the action of similar residual impurities in the basic substance, having the same retarding growth effect. It is interesting to note that ethylene-glycol "impurity" increases the overall growth rates, probably due to complex formation with the residual impurities of the Me^{3+} type, which have a weaker action in the adsorbed layer.

4. Surface 2D - nucleation mechanism of growth

In order to check the surface nucleation mechanism, we have used the concept of two-dimensional (2D) - nucleation, as introduced by Chernov [31,32]. The experimental data R(σ) of the three kinetic curves from Fig. 2, were represented in Fig. 4 as:

$$\ln \frac{R}{\sigma^{5/6}} = \ln A - \frac{B}{\sigma} \tag{2}$$

The values of B constant are given in Table 2. They were found from the fit of this equation at higher supersaturations, by the least square method. The edge free energy ratio γ / kT and α the surface energy of 2D nucleus ($\gamma\, \bar{a} = \alpha\, \omega$), were found in Table 3, according to equation:

$$B = \frac{\pi}{3}\left(\frac{\gamma}{kT}\right)^2 = \frac{\pi}{3}\left(\frac{\alpha\sqrt{\Omega\, d}}{kT}\right)^2 \tag{3}$$

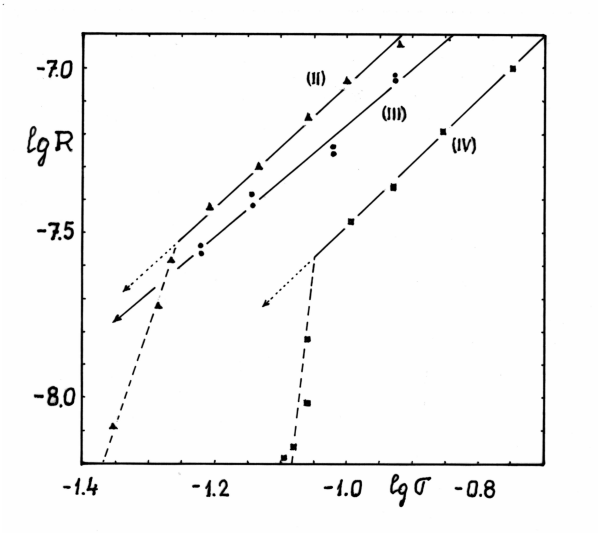

Fig. 3. Kinetic data from Fig. 2, in double log coordinates.

Table 2. Constants of 2D nucleation mechanism of growth for reduced rate at 40 °C.

Curve Fig.1	T (°C)	pH	$A^{40\ °C}$ *)	B	r (%)
(II)	30	N	$2.11_8 \times 10^{-6}$	7.50×10^{-2}	99.5
(III)	52	4.8	$0.66_5 \times 10^{-6}$	7.73×10^{-2}	99.4
(IV)	40	N	$0.94_5 \times 10^{-6}$	14.6×10^{-2}	99.2

*) Constants in eq. (5) are: $C_e^{40^\circ C} = 1.29_7\ 10^{27}$ (molec/m^3) and $\beta_\ell^{40\ °C} = 1.34_8\ 10^{-3}$ m/s

The values of A constant, found according to eq.(2) at several temperatures, were Arrhenius corrected with the activation energy of 9.5 kcal/mol [14] and are also given in Table 2 as $A^{40\ °C}$. Using these standard values, the surface density of ad-molecules capable to initiate de surface nucleation was calculated according to equation [31,32]:

$$n_S = \frac{\left(A / C_e \beta_\ell\right)^3}{\omega^2\, d^4\, \bar{a}} \tag{4}$$

and are given in Table 3.

The following characteristic data of the KDP crystal have been used:

- the tetragonal X-ray cell, with 4 chemical formula have the dimensions: $a_1 = a_2 = 7.43_5 \times 10^{-10} m$, $c = 6.95_9 \times 10^{-10} m$ and the volume of the growth unit (GU): $\Omega = a_1 a_2 c / 4 = 96.17_2 \times 10^{-30}\ m^3$,
- the elementary step height: $d = a_2 / 2 = 3.71_{75} \times 10^{-10} m$
- the medium dimension of the GU on the prismatic face: $\bar{a} = \sqrt{2\Omega / a_2} = \sqrt{a_1 c / 2} = 5.08_6 \times 10^{-10} m$

and the following kinetic data in the equation of step motion [7]:

$$v = \beta_\ell C_e \Omega \sigma \tag{5}$$

- the volume concentration of solute molecules in the saturated solution: $C_e = (X / M_{KDP}) N_{Av} [100 + X / \rho_{KDP}]^{-1}$, according to the solubility curve X(g KDP/100 g H_2O).
- the kinetic coefficient of steps $\beta_\ell^{40\ ^oC} = 1.34_8 \times 10^{-3}$ m/s, calculated using $\beta_\ell^{38\ ^oC} = 1.22 \times 10^{-3}$ m/s and the activation energy of ~ 9.7 kcal/mol [11].

Using the surface density of native molecules (GU): $n_0 = 2 / a_1 c = (\bar{a})^{-2} = 3.86_5 \times 10^{18} m^{-2}$ on the prismatic faces of the crystal, the surface coverage of ad-molecules susceptible to trigger 2D nucleation $\theta = n_s / n_0 \sim 10^{-6}$ was estimated in Table 3.

Table 3. Essential parameters estimated from 2D nucleation model.

Curve Fig.1	γ / kT	α (mJ/m^2)	$10^{-12} \cdot n_s^{40\ ^oC}$ (m^{-2})	$\theta^{40\ ^oC}$	σ^* (%)	$\theta^* = \frac{n_s^*}{n_o}$
(II)	0.26_8	5.9_2	19.7_9	$5.12_0\ 10^{-6}$	2.8	$2.73\ 10^{-3}$
(III)	0.27_2	6.4_1	0.61_1	$0.15_8\ 10^{-6}$	1.6	$0.86_5\ 10^{-3}$
(IV)	0.37_3	8.5_3	1.75_6	$0.45_4\ 10^{-6}$	6.4	$7.36\ 10^{-3}$

Note: critical supersaturation at the limit of the "dead" growth zone σ^* and the critical coverage θ^* substantially decreases with the pH increase.

The critical supersaturation σ^* at the limit of the "dead" growth zone, given in Table 3, was used in order to estimate the surface critical coverage of impurities:

$$\theta^* = \frac{n_s^*}{n_0} = \left[\frac{\gamma}{kT}\frac{2}{\sigma^*}\right]^{-2} \tag{6}$$

This critical coverage of impurities was estimated according to the Cabrera-Vermilyea concept [33], when the growth of the face is stopped at critical supersaturation σ^*. The density of ad-molecules $n_s^* \approx (2\rho_c^*)^{-2}$ was considered at the critical stages, when the mean distances between the stopper impurities are comparable with the diameter of the critical nucleus: $2\rho_c^* = 2(\gamma / kT) \cdot (\bar{a} / \sigma^*)$. The surface critical coverage $\theta^* \sim 10^{-3}$ in table 3, are in good agreement with some other data found by Alexandru [20].

In the transient region at lower supersaturations, near the "dead" growth zone, the equivalent data for curves (II) and (IV) are given in table 4. The edge free energy ratio γ / kT = 0.43 for curve

(II) in Table 4, agree with the value 0.42÷0.47 found by Alexandru [14,20] and is close to 0.40 value, estimated by Sőhnel et al [34]. However, the coverage of ad-molecules susceptible to trigger the 2D nucleation mechanism $\theta^{40\ ^{o}C} = 2.2 \times 10^{-3}$ for curve (II), appears to be much too smaller versus the density of native GU in the adsorbed layer (θ is expected to be at lest of a few percent). For the curve (IV) the coverage $\theta > 1$ suggests the nucleation model is inadequate [14].

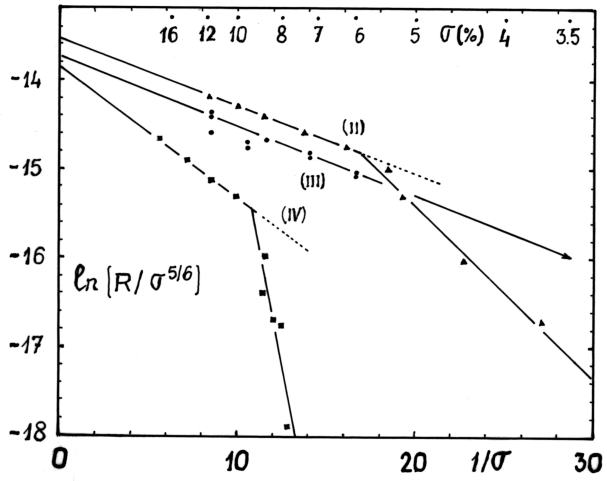

Fig. 4. Kinetic data from Fig. 2, in coordinates of 2D nucleation mechanism of growth. Characteristic data for the three experiments are presented in tables 2 and 3. Constants A and B were calculated by the least square method with the correlation factor r(%) given in Table 2.

5. Discussion

On the dislocation free (101) crystal surfaces of ADP (isomorphous to KDP), Malkin et al. [31,32] have measured the growth rate produced by 2D nucleation mechanism. The growth rate ensured by this 2D-nucleation mechanism exceeds the dislocation growth rate only at $\sigma \geq 8$ %. This limit is about the same (6÷8 %) as those estimated by Alexandru et al [14] for prismatic faces of KDP. The dislocation mechanism of growth appears dominant at smaller supersaturations, where the dislocations spontaneously "burst" and ensures higher growth rates [31]. At very small supersaturations, on very carefully dislocation free "regenerated" surfaces [31,32], a heterogeneous 2D-nucleation mechanism of growth on impurities (with a surface energy $\alpha = 4.2$ mJ/m^2) was found to be active. At higher supersaturations $\sigma > 4 \div 5$ % a homogeneous 2D-nucleation mechanism (with a surface energy $\alpha \approx 12$ mJ/m^2) was found to be active [31,32].

In ex-situ AFM studies of pyramidal faces of KDP, grown from solutions in defined conditions, De Yoreo et al [35] have shown that at $\sigma \sim 8 \div 10$ % the growth occurs both on dislocation induced steps and on the steps of islands formed by 2D-nucleation. Dislocation mechanism of growth is certainly dominant at supersaturations below 5 %. The nucleation occurred on the interstep terraces larger than the diffusion length of the GU ($\lambda_s \approx 250$ nm) on the crystal face. It was noticed that if the growth of a step becomes impeded, 2D nuclei would rapidly cover the adjacent terrace in front of the step [35].

The well known harmful impurities Cr^{3+}, Fe^{3+}, Al^{3+} as previously shown [20], have a dual action in crystal growth. Such impurities, having a long residence time in the adsorbed layer, become stoppers for the elementary steps and at higher supersaturations enhance the surface heterogeneous nucleation rate.

We shall further discuss the growth kinetic curve (II) from Fig. 2. The explanation of the "dead" growth zone might be the following. In impure solutions at low supersaturation, "poison" impurities Me^{3+} having a long residence time in the adsorbed layer, behave as a "forest" of stoppers for the layers produced by the dislocation mechanism. At supersaturations higher than the critical ones

σ^* ~ (2÷3) %, the heterogeneous nucleation at some locally adsorbed impurities, start to become active and fluctuating velocities of the layers, squeezing among the stoppers, give rise to an increasing growth rate of the crystal, in the intermediate growth range up to σ ~5%. At higher supersaturations $\sigma \geq$ (5÷6) %, as previously shown [35], homogeneous 2D–nucleation become increasingly important versus the heterogeneous one and compete the dislocation mechanism. However, in the impurified solutions, in the higher supersaturation range, where homogeneous nucleation would have to be dominant, the estimated surface energy $\alpha \approx$ (5.9÷8.5) mJ/m^2 (Table 3) is intermediate between 4 and 12 mJ/m^2 corresponding to heterogeneous and homogeneous 2D-nucleation respectively, as measured by Malkin et al. [31,32] for ADP. On the other hand, the surface coverage of ad-molecules $\theta^{40\ ^oC} \sim 10^{-6}$ (Table 3), which is about of the same order of magnitude as impurity concentration in solution, suggests the heterogeneous nucleation mechanism is dominant for KDP crystal. However, on the whole range of supersaturations, adsorbed impurities still act as layers stopper and the overall growth rate is smaller than in pure solution.

At higher concentration of impurities the retarding effect increases at all supersaturations. The concentration of adsorbed impurities (coverage) essentially depends on the time during which the impure solution "see" the fresh terraces between two successive moving steps. Thus, the concentration of impurities in the adsorbed layer and in the crystal depends, through a feedback effect, on the growth rate, i.e. on supersaturation and the overall concentration of impurities in solution. The shape of R(σ) curves at higher impurification is more or less similar to those of lower impurification, but curves are shifted towards the higher supersaturations and the "dead" growth zone are extended (see curve (IV) in Fig. 2).

In the transient region, at lower supersaturations, the parameters estimated in Table 4 do not have a real support in the 2D-nucleation mechanism of growth. In this region the dislocation mechanism of growth is "obscured" by the layers retarding effect of the stopper impurities. The critical coverage $\theta^* \sim 10^{-3}$ (Table 3), at the limit of the "dead" growth zone, shows the stopper action of impurities prevails. In the supersaturation range of active growth, the coverage of ad-molecules vary three order of magnitude ($\theta^{40\ ^oC} \leftrightarrow \theta^*$ in Table 3), suggesting the segregation coefficient is also very large at smaller supersaturations. This fact points to an extremely important practical conclusion: the crystal purity might increase at higher rate of growth. This observation is in stark contrast with the segregation of impurities in crystals grown from the melt [36].

Table 4. Parameters estimated from 2D nucleation model for the transient region at lower supersaturations.

Curve Fig.1	$A^{40\ ^oC}$ (m/s)	γ / kT	n_s (m^{-2})	$\theta^{40\ ^oC}$
(II)	$1.61_0 \times 10^{-5}$	0.43_0	$8.6_9 \times 10^{15}$	$2.2_5 \times 10^{-3}$
(IV)	$1.17_1 \times 10^{-2}$	0.98_7	$3.3_4 \times 10^{24}$	$8.6_5 \times 10^{5}$

The influence of solution pH on the shape of the kinetic curves is quite obvious in Fig. 2 (curve III), in Fig. 4 and in Table 3. As a result of pH increase from normal value (~ 4) to 4.8, the extension of the "dead" growth zone σ^* and the corresponding critical coverage θ^* in Table 3 substantially decrease. For the curve (III) in Figs. 2 and 4 the intermediate growth zone tends to "normal", although the retarding effect of impurities on the whole curve is still visible. It seems that the increased concentration of hydroxyl group make some complexes with Me^{3+} impurities, changing theirs adsorption energy in the surface layer.

A minimum value of this adsorption energy can be estimated, if we consider τ the life time of impurities in the adsorbed layer, comparable to the time interval $t_1 = d / R$ between two successive steps crossing a point on the crystal surface. Thus, from equation:

$$\frac{d}{R} \approx \tau = (kT/h)^{-1} \exp(E_{ads}/kT) \quad (7)$$

we have found for several growth rates in table 5 the values (15÷18) kcal/mol, which are considerably higher than ~ 9 kcal/mol [37,38], the activation energy for growth, i.e. the dehydration barrier of the GU in the BCF surface diffusion model [30].

Bredihin et al [17] have found the adsorbtion energy of ~15 kcal/mol for Al^{3+} and Fe^{3+} on the (100) type faces of KDP crystal. Chernov and Malkin estimated activation energy as large as 24 kcal/mol of impurities on the pyramidal faces of ADP [39,40]. The "life" time in the adsorbed layer for such impurity is of the order $\tau \sim 5\times10^4\, s$, i.e. much larger than $t_1 \sim (10^{-3}\div10^{-1})$ s in our experiments. Such impurities are certainly engulfed in the crystal and decrease the technological parameters of the usable crystals.

Table 5. Adsorption energy of impurities

σ	0.03	0.05	0.10
R (m/s)	10^{-9}	$3\ 10^{-8}$	10^{-7}
τ (s) = d / R	1/2	1/60	1/200
E_{ads} (kcal/mol)	17.9	15.8	15.0

6. Conclusions

Growth kinetic of prismatic faces of KDP crystal in impurified solutions (Fe^{3+}) was measured and analyzed. Surface 2D-nucleation mechanism was found to apply at higher supersaturations, but the estimated surface energy $\alpha \approx (6\div8)$ mJ/m^2 is smaller than $\alpha \approx 12$ mJ/m^2 found for homogeneous nucleation of ADP, isomorphous to KDP [31,32]. In this ranges of supersaturation the estimated coverage $\theta\sim10^{-6}$ (Table 3) of adsorbed molecules, susceptible to trigger the surface nucleation is about of the same order of magnitude as impurity concentration in solution. Both facts suggest a heterogeneous 2D-nucleation mechanism being dominant.

The lower limit of the adsorbtion energy of Fe^{3+} impurity (15÷18) kcal/mol, we have estimated on the prismatic faces of KDP, is very close to ~ 15 kcal/mol value estimated by Bredihin et al [17] from other type of measurements. This energy is much larger than ~ 9 kcal/mol, the activation energy for growth [37,38]. Chernov and Malkin [39,40] have found the adsorption energy of ~ 24 kcal/mol for the same type of impurities on the pyramidal faces of ADP. These figures suggest the Me^{3+} impurities have a long life in the adsorbed layer and usually are engulfed in the crystal.

According to some other literature data [14,20,31,32,35] the dislocation mechanism of growth is dominant up to supersaturations of $\sigma \sim (8\div10)$ %. Nevertheless, in impure solutions the retarding effect of "poison" impurities of Me^{3+} type, drastically changes the growth kinetic curves.

At the limit of the "dead" growth zone, the critical coverage $\theta^* \sim10^{-3}$ is about three order of magnitude higher than $\theta\sim10^{-6}$ (Table 3), estimated at higher supersaturations. This fact suggests that the segregation coefficient of Me^{3+} impurities decreases considerably at higher supersaturations (and higher growth rates), being in stark contrast with the behavior of the segregation coefficient in crystals growth from melt [36].

It has been shown that the increase of the solution pH changes the shape of the growth kinetic curves and possibly the segregation coefficient of impurities.

References

[1] T. Sasaki, A. Yokotani, J. Crystal Growth **99**, 820 (1990).
[2] N. P. Zaitseva, F. S. Ganihanov, O. V. Kachalov, V. F. Efremov, S. A. Bastuhov, V. B. Sobolev, Kristallografyia **36**, 1231 (1991).

[3] N. P. Zaitseva, J. J. De Yoreo, M. R. Dehaven, R. L. Vital, K. E. Montgomery, M. Richardson, L. J. Atherton, J. Crystal Growth **180**, 255 (1997).
[4] J. J. De Yoreo, B. W. Woods, J. Appl. Phys **73**, 7780 (1993).
[5] J. J. De Yoreo, Z. U. Rek, N. P. Zaitseva, B. W. Woods, J. Crystal Growth **166**, 291 (1996).
[6] N. P. Zaitseva, J. Atherton, R. Rozsa, L. Carman, I. Smolsky, M. Runkel, R. Ryon, L. James, J. Crystal Growth **197**, 911 (1999).
[7] A. A. Chernov, L. N. Rashkovich, J. Crystal Growth **84**, 389 (1987).
[8] A. A. Chernov, L. N. Rashkovich, A. A. Mkrtchyan Kristallografyia **32**, 737 (1987).
[9] A. A. Chernov, A. I. Malkin, I. L. Smol'skii, Kristallografyia **32**, 1502 (1987).
[10] A. A. Chernov, L. N. Rashkovich, I. L. Smol'skii, Yu. G. Kuznetsov, A. A. Mkrtchan, A. I. Malkin, Growth of Crystals vol. 15, s. E. I. Givargizov, S. A. Grinberg, Consultants Bureau N.Y., London 1988.
[11] A. A. Chernov, Z. Phys. Chemie, Leipzig **269**, 941 (1988).
[12] A. A. Chernov, Contemporary Physics **30**, 251 (1989).
[13] H. V. Alexandru, J. Crystal Growth **205**, 215 (1999).
[14] H. V. Alexandru, C. Berbecaru, Al. Grancea, V. Iov, J. Crystal Growth **166**, 162 (1996).
[15] H. V. Alexandru, C. Berbecaru, 14-th Internat. Symp. on Industrial Crystallization, 12-16 sept.1999, Cambridge, UK, Proceedimgs 282 (3).
[16] H. V. Alexandru, Internat. Conf. Crystal Growth - ICCG XIII, Kyoto, Japan, Aug 4, 2001, A 0424.
[17] V. I. Bredihin, V. I. Ershov, V. V. Korolihin, et al Kristallografyia **32**, 214 (1987).
[18] I. Owczarek, K. Sangwal J. Crystal Growth **99**, 827 (1990).
[19] S. P. Kuz'min, V. A. Kuznetsov, T. M. Ohrimenko, H. S. Bagdasarov, Kristallografyia **39**, 914 (1994).
[20] H. V. Alexandru, Cryst. Res. Technol. **30**, 1071 (1995).
[21] G. Endert, M. L. Martin, Cryst. Res. Technol. **16**, K65-K66 (1981).
[22] C. Belouet, E. Dunia, J. F. Petroff, J. Crystal Growth **23**, 243 (1974).
[23] A. V. Belustin, A. V. Kolina, Kristallografyia **20**, 206 (1975).
[24] A. V. Belustin, A. V. Kolina, Kristallografyia **23**, 230 (1978).
[25] J. J. De Yoreo, T. A. Land, B. Dair, Phys. Rev. Letters **73**, 838 (1994).
[26] H. V. Alexandru, A. C. Otea, G. Hlevca, Rev. Roum. Phys. **30**, 525 (1995).
[27] H. V. Alexandru, C. Berbecaru, Cryst. Res. Technol. **30**, 307 (1995).
[28] H. V. Alexandru, C. Berbecaru, B. Logofatu, A. Stanculescu, F. Stanculescu, J. Optoelectron. Adv. Mater. **1**, 57 (1999).
[29] H. V. Alexandru, Anal. Univ. Buc. **46** (1997) 9-16, Proceedings ROCAM '97 conference.
[30] W. K. Burton, N. Cabrera, F. C. Frank, Phil. Trans. Roy. Soc. **A 243**, 199 (1951).
[31] A. I. Malkin, A. A. Chernov, I. V. Alekseev, Kristallografyia **34**, 968 (1989).
[32] A. I. Malkin, A. A. Chernov, I. V. Alekseev, J. Crystal Growth **97**, 765 (1989).
[33] N. Cabrera, V. A. Vermilyea, Growth and perfection of crystals, New York 1958, pag. 393.
[34] O. Sőhnel, J. Garside, S. J. Jancik, J. Crystal Growth **39**, 307 (1977).
[35] J. J. De Yoreo, T. A. Land, B. Dair, Phys. Rev. Lett. **73**, 838 (1994).
[36] J. A. Burton, R. C. Prim, W. P. Slichter, J. Chem. Phys. **21**, 1987 (1953).
[37] H. V. Alexandru, J. Crystal Growth **169**, 347 (1996).
[38] P. G. Vekilov, Yu. G. Kuznetsov, J. Crystal Growth **119**, 248 (1992).
[39] A. A. Chernov, A. I. Malkin, I. L. Smol'skii, Kristallografyia **32**, 1508 (1987).
[40] A. A. Chernov, A. I. Malkin, Kristallografyia **33**, 1487 (1988).
[41] J. W. Mullin, A. Amatavivadhana, J. Appl. Chem. **17**, 151 (1967).
[42] R. J-van Rosmalen, W. H. van der Linden, E. Dobinga, D. Visser Kristall u Technik **13**, 17 (1978).